DOI: 10.2478/rjti-2024-0018
ROMANIAN JOURNAL
OF TRANSPORT INFRASTRUCTURE

FEXIBILITY OF BRIDGES BUILT USING THE CANTILEVER METHOD

Czesław Machelski- Prof. PhD Eng., University of Science and Technology, Department of Bridge and Railway, Wroclaw, czeslaw.machelski@pwr.edu.pl
Bartosz Pisarek- MSc Eng., Wayss & Freytag Ingenieurbau AG bartosz.pisarek@wf-ib.de

Abstract

The cantilever concreting technology is one of modern methods of constructing the concrete long-span bridges. The fundamental features of this method are saving of materials and of construction costs (especially of scaffolding and of formwork) and first of all a possibility of carrying out the construction of the span in many spots at the same time. The negative feature of these bridges is a large long-term deflection of the bridge, as a result of rheological processes in the concrete and in the pre-tensioning steel. Deflection measurements at the mid-span indicate a visible lowering of the grade line of the bridge span, already after few years of service. The calculated flexibility can be useful in analyses of long-term (rheological) changes in concrete bridge structures. It is a complement to the term bridge stiffness used in the case of momentary (short-term) loads, including dynamic actions.

Keywords: cantilever bridges, rheology, deflection, construction, calculation

1. INTRODUCTION

Concrete bridges with long spans, built using the cantilever method [9, 13, 17, 18] are analysed in this paper and have a characteristic appearance (Figure 1). The changes in their height and the geometric parameters of their cross section were adjusted to the construction method.

The cantilever system and the loading configuration adopted at the construction stage [13] cause the classic structural system in the form of a tapered box girder as shown in Figure 1.

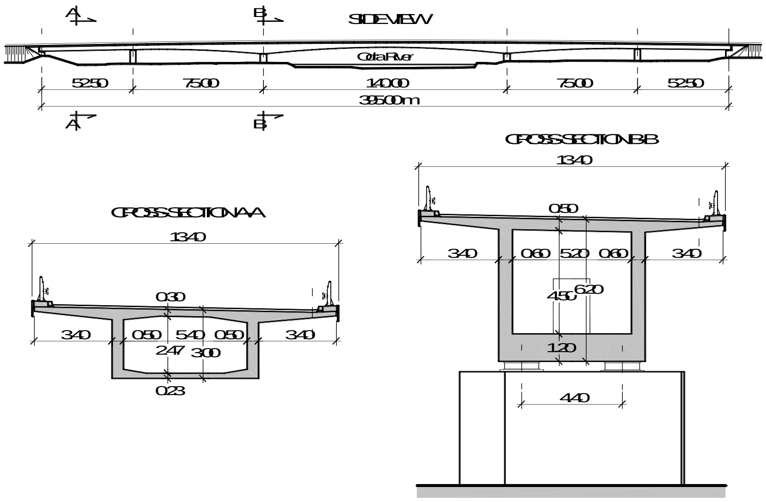

Figure 1. Geometry of Kędzierzyn-Koźle bridge [9].

The analysis assumes, that the dead load resulting from the cross-sectional area changes only to a limited extent. The weight of the secondary components in this case is identical along the whole length of the bridge. The overall result of the loads is a uniformly distributed force with magnitude q.

In some bridges built using the cantilever -cast-in-place segmental construction- method the increasing deflections of the span are of major significance [2, 6, 7, 8, 9, 10, 11, 19, 20], as in the example shown in Figure 2. This phenomenon often occurs in the case of a triple-span structural system with the short spans adjoining the main span [3, 4, 13].

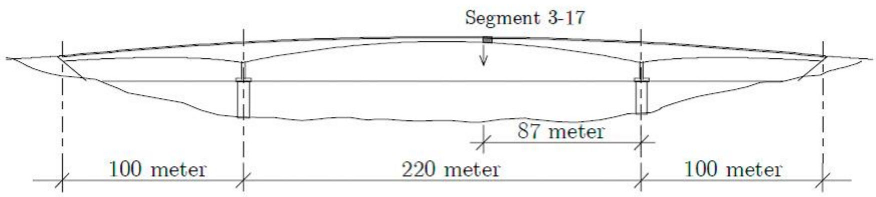

Figure 2a. Increment in in-service deflections of Støvset bridge [8, 13].

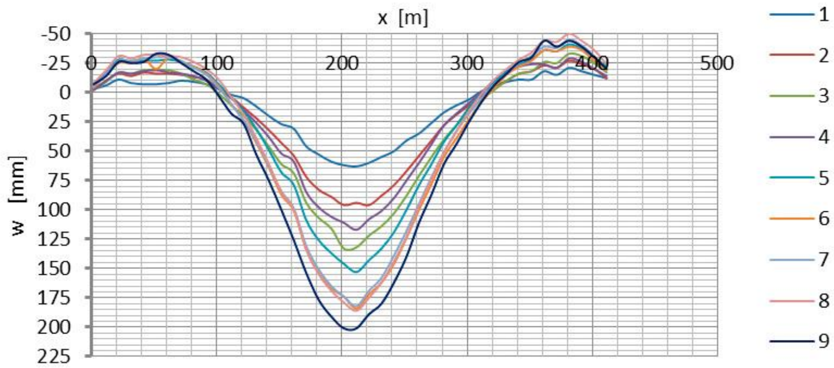

Figure 2b. Increment in in-service deflections of Støvset bridge [8, 13].

The numbers of the time intervals between the reference measurement (0) and the analysed measurements (1-9) are given in the diagram's legend (Figure 2b). The bridge was built in October 1993 and the reference measurement was taken on 22.02.1994 on the last in the 2001 (Table 1) [17]. Corresponding to that results (Table 1) the deflection in the middle of the span between the first (0) and the last (9) measurement is like ca. 150mm.

Table 1. Times at which Støvset bridge grade line measurements were taken

Number	0	1	2	3	4	5	6	7	8	9
Year	1994	1994	1995	1996	1996	1997	1998	1999	2000	2001
month	02	07	08	06	10	06	06	06	06	06
Day	22	07	15	04	02	25	16	23	21	13

In this case is taken, that this change (progress) of deflection results from the rheological processes, which are principal determined by the uniformly distributed force (permanent load) q [13, 19, 21]. This corresponds to the two major factors:

- the structural system, and
- the distribution of stiffness along the span.

In the further part of the paper will be showed, that the flexibility of the object corresponds to those major principles and can be useful in analyses of long-term (rheological) changes in concrete bridge structures.

2. CHARACTERISTIC DISPLACEMENTS OF INTERIOR SPAN

An example bridge (Figure 2) with a structural arrangement and deformation as shown in Figure 3 is considered below. Assuming the structure and the load to be symmetrical and considering the line of deflection of the spans, a half of the structure was used in the computational model. The displacement method [13] was applied to the model. Deflection w and two angles of rotation φ and ψ over the supports were the sought quantities. The main problem is the deformation of the main span with length $L = 2a$. The spans are loaded with a uniformly distributed force with magnitude q.

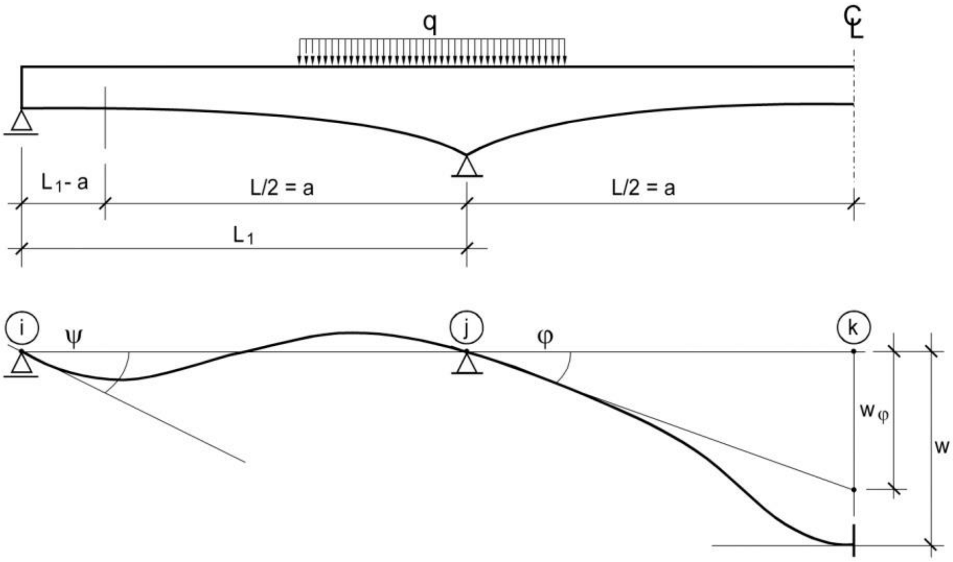

Figure 3. Deflection line with characteristic displacements of spans

In terms of parameters, the computations yield the deflection at the mid span of the main span

$$w = c_W \cdot \frac{qa^4}{EI} \tag{1}$$

where: w – deflection of the mid span
q – uniformly distributed force
a – half of the span length (L)
E – Young-modulus
I – moment of inertia,

and angle of rotation φ from which the value of w_φ shown in Figure 3 is calculated as follows

$$w_\varphi = \varphi \cdot a = c_F \cdot \frac{qa^4}{EI} \tag{2}$$

where: w_φ – deflection of the mid span from the rotation of the span
φ – angle of rotation
a – half of the span length (L)
q – uniformly distributed force
E – Young-Modulus
I – moment of inertia,

In formulas (1) and (2) EI stands for bending stiffness at the mid span of the main span, i.e. in node k and over support i of the end span. For the calculations the moment of inertia was assumed to change parabolically in the segment between nodes j and k, identically as in the adjacent segment with length a. A constant part occurs in both the displacements. Quantities w and c fare the variables in this solution. Further in this paper they will be referred to as the results of the parametric analysis. They are characteristic quantities representing the deformation of the interior span as shown in figures 1, 2 and 3. The value of c_F indicates the contribution of over-support angle of rotation φ to the deflection at the mid span of the main span. This deflection is of major significance, as demonstrated by exemplary analyses and test results [13] and also in Figure 2.

3. MOMENT OF IERTIA FUNCTIONS

Many factors are considered when selecting the lower line of the span structure. One of them are the bridge's aesthetic qualities [6]. The designed appearance (shape) of the bridge is determined by the kind of material used for the reinforced concrete or prestressed concrete structure and by the construction method [1] In the case of long-span concrete bridges, also the length (L) of the main span has a bearing on the height proportions. Consequently, moment of inertia functions $I(x)$ differ between bridges.

The coefficients of stiffness were calculated using changes in moments of inertia in the form of the function

$$I(x) = I\left[1 + \left(\sqrt[3]{n} - 1\right)\left(\frac{x}{a}\right)^2\right]^3 \tag{3}$$

where: I – moment of inertia
n –stiffness ratio
a – half of the span length (L)

where n is defined by the stiffness ratio

$$n = \frac{I_k}{I_j} = \frac{1}{7.8} \tag{4}$$

where: n –stiffness ratio
I – moment of inertia,

while the location of the section is expressed as *x/a*.

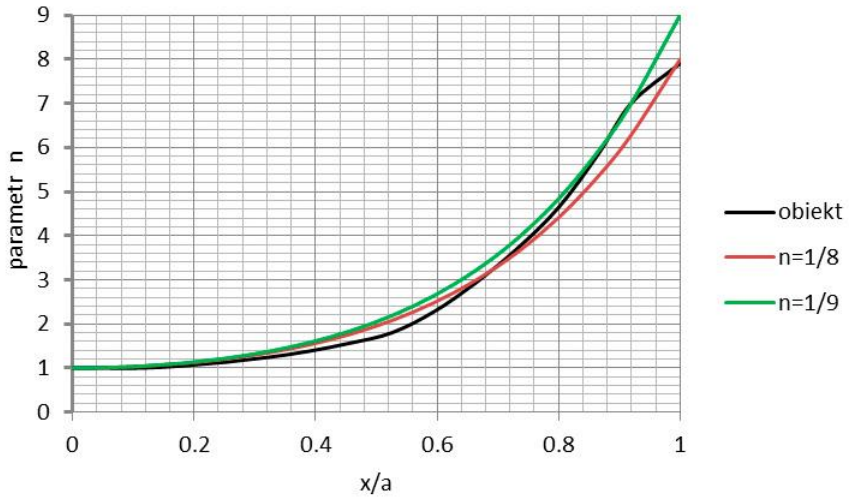

Figure 4. Moment of inertia functions

Figure 4 shows the shapes of function $I(\xi)$ when n = 1/8 and n = 1/9. The graphs were compared with the results obtained on the basis of the cross-sectional geometry of the bridge shown in Figure 1. The comparison shows a good fit between the respective functions. Direct calculations, in which the design moments of inertia are used, yield overrated results.

4. DEAD LOAD FUNCTIONS

In bridges built using the cantilever method the cross-sectional area changes regularly, as a result of initially changes in height and then changes in the thickness of the bottom slab of the bridge. Figure 5 shows how dead load g(x) changes relative to its value in the key (g_k) as in the formula

$$r(x) = \frac{g(x)}{g_k} = \frac{A(x)}{A_k} \tag{5}$$

where: *r(x)* – relationship between unit strains ε(t) and normal stresses σ(t),
g – dead load
A – area of the cross-section

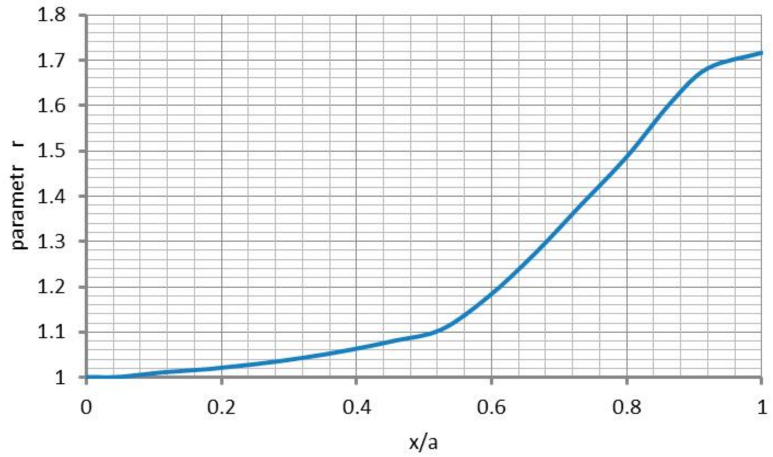

Figure 5. Dead load function.

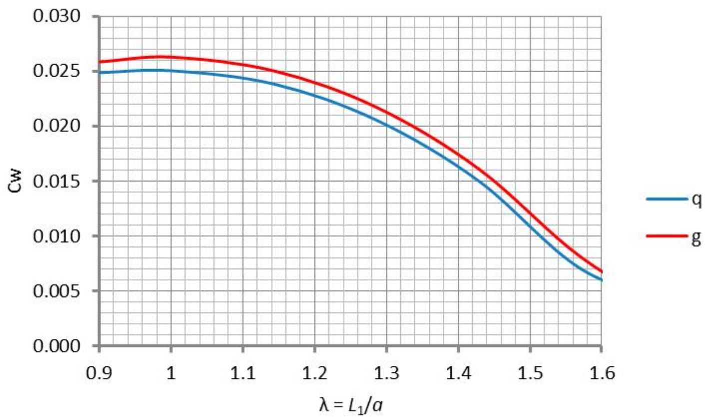

Figure 6. Parameter c_w versus end span lengthL1.

The calculation results for the bridge as in Figure 3 when n = 1/8 and the variable parameter is L_1/a are compared in Figure 6. The comparison of the two curves shows that they fully agree with relation g/q = 1.05 when $L_1=a$ and relation g/q = 1.09 when L_1 = $3a/2$. Thus the results reported further in this paper for uniformly distributed load q can be regarded as applying to dead load g.

5. TRIPLE-SPAN BRIDGE CONFIGURATION

An example bridge structure as in Figure 2, whose load diagram is shown in Figure 3, is considered below. End span length L_1 = a was assumed in the calculations. Thus, the structural system consists of two identical parts (repeated symmetrically on the other side of the computational model). The variable in this analysis is the bending stiffness ratio in nodes *j* and *k*, as the parameter

$$n = \frac{EI_k}{EI_j} = \frac{EI}{EI_j} \tag{6}$$

where: n- bending stiffness ratio
E – Young Modulus
I – moment of inertia,

The change in stiffness along a segment with length a is discussed in the next section of this paper.

Figure 7 shows the calculation results in the form of parameters *c* contained in formulas (1) and (2). The diagram's legend shows subscripts *w* and *F* from the formulas. The range of change in parameter *n* applies not only to bridges built using the cantilever method, but also to bridges with a constant cross section when *n = 1*. Intermediate cases are applicable to any bridges. There are no constraints imposed on interior span length *L* (and the length of the end spans: $L_1 = a$).

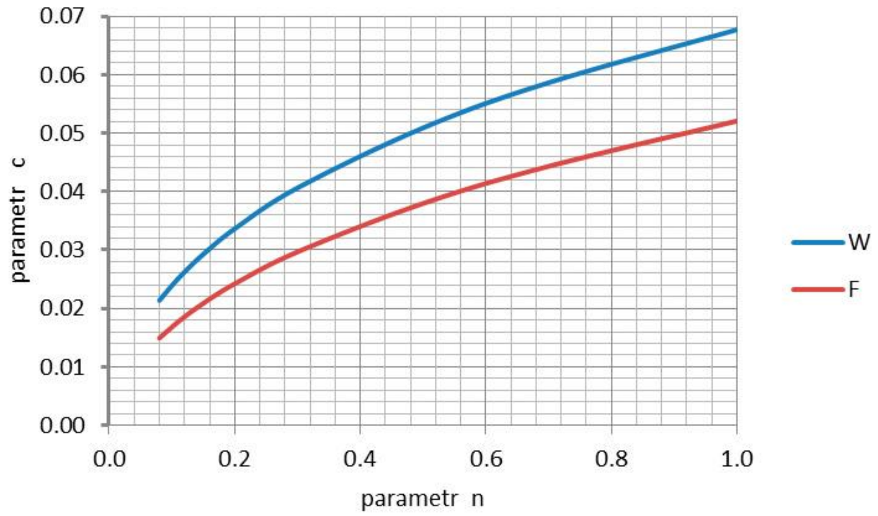

Figure 7. Displacements versus stiffness in intermediate pier zone.

The graphs show *a* considerable reduction in displacements in the case of spans with haunches. The high value of the angle of rotation over the intermediate pier is of major significance here. This is consistent with the measurement results presented in Figure 2. In the special case of a beam with a constant moment of inertia when *n = 1*, one gets

$$w = \frac{13}{192} \cdot \frac{qa^4}{EI} \tag{7}$$

where: *w* –deflection of the mid span
a – half of the span length (*L*)
E– Young Modulus ,
I – moment of inertia,

and

$$\varphi = \frac{10}{192} \cdot \frac{qa^3}{EI} \tag{8}$$

where: φ – angle of rotation
q – uniformly distributed force

Thus, the main cause of the considerable deflection is angle of rotation φ, as in Figure 3. For comparison when $n = 0.12$, one gets much lower values

$$w = \frac{5.03}{192} \cdot \frac{qa^4}{EI} \tag{9}$$

where: *w*- deflection of the mid span
q – uniformly distributed force
E – Young Modulus ,

and

$$\varphi = \frac{3.57}{192} \cdot \frac{qa^3}{EI} \tag{10}$$

where: φ – angle of rotation
q –uniformly distributed force

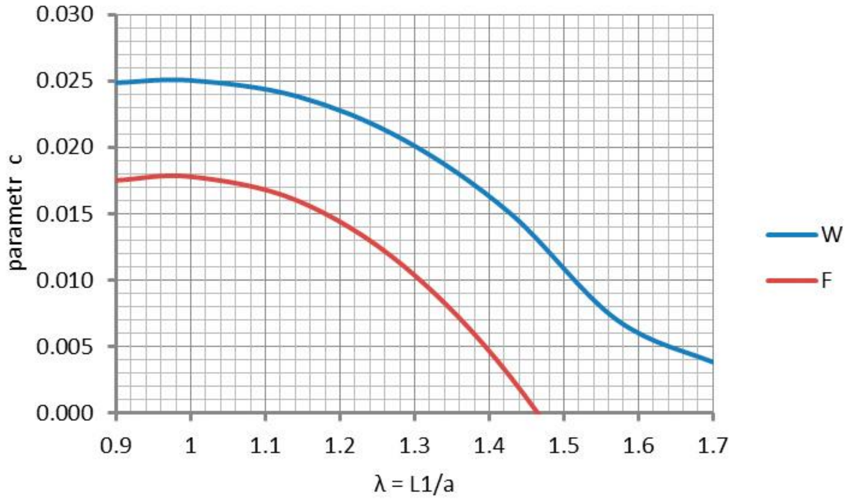

Figure 8. Displacement versus end span length $L_1/a = \lambda$. (parameter)

The calculation results for $n = 1/8$ are presented in Figure 8. When $\lambda = 1$, the result is consistent with the diagram shown in Figure 7. When $\lambda > 1$, a half of the end span is parabolically hunched (as between nodes j and k), whereas the remaining part has a constant height, as in Figure 3. The diagram's legend shows subscripts W and F from formulas (1) and (2). The graphs (Figure 8) show a considerable reduction in angle of rotation φ with increasing span length L_1 and the resulting considerable changes in deflection. In the example given in Figure 2 there is ratio $L_1/a = \lambda = 0.91$. It appears from the diagram shown in Figure 8 that this results in considerable deflections and a considerable angle of rotation. Therefore, to limit the deflection of the interior span it is important to use ratio $L_1 > 5a/4$.

A negative example of the propagation of excessive deflection is the Koror-Babelthaupt bridge (Figure 9) with span length $L = 241m$ and very short end spans L_1 at $\alpha \approx 0.4$ [1, 12, 19]. After 12 years of service life the displacement amounted tow = 1.2 m. After 18 years of service life, it increased to $w = 1.39$ m and repeatedly exceeded the allowable value. The strengthening of the structure by means of a secondary prestress ended in failure and after a short in-service period in a collapse. A detailed analysis of this case was presented in [18].

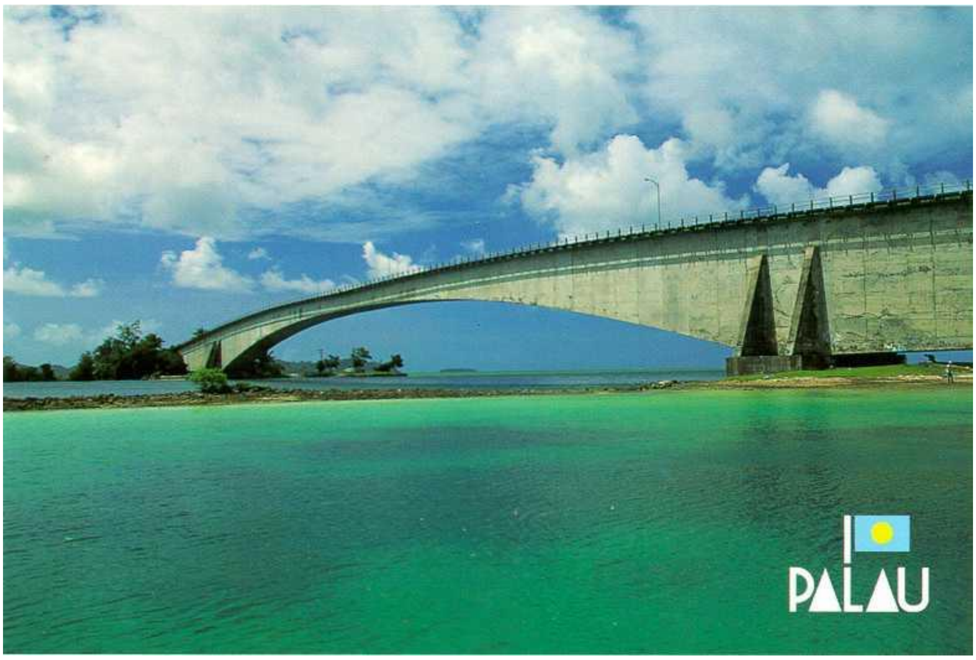

Figure 9. View of Koror-Babelthaupt bridge.

6. FIVE-SPAN BRIDGE CONFIGRATION

Previously the bridge structural system was considered in a triple-span configuration as shown in Figure 2 and 3. Figure 1 shows a symmetrical five-span bridge configuration. In this case the end spans have a constant length (and a constant moment of inertia). In the formulas the lengths of the end spans *(*L_2) relative to the main span are expressed by the parameter

$$\beta = \frac{L_2}{a} = \frac{2 \cdot L_2}{L} \tag{12}$$

where: a – half of the span length (L)
L – bridge span

The calculation results for the bridge configuration as in Figure 1 are presented in Figure 10. Span length ratio $L_2/L_1 = 0.7$ was kept constant. Thus in this calculation example both a and β are variables, but at constant proportion $\beta = 0.7a$. The results presented in Figure 8 indicate an increment in main span deflections, caused by the appearance of a deflection directed upwards the intermediate span. This applies to the case of short span lengths L_1 and L_2. Therefore, the consequence of the adoption of a five-span system is an increment in the deflection of the main span. This also applies to multi-span systems. If the length of the intermediate span increases considerably, i.e. when $L_1 > 5a/8$, a considerable reduction in deflection occurs, similarly as indicated by the results presented in Figure 8.

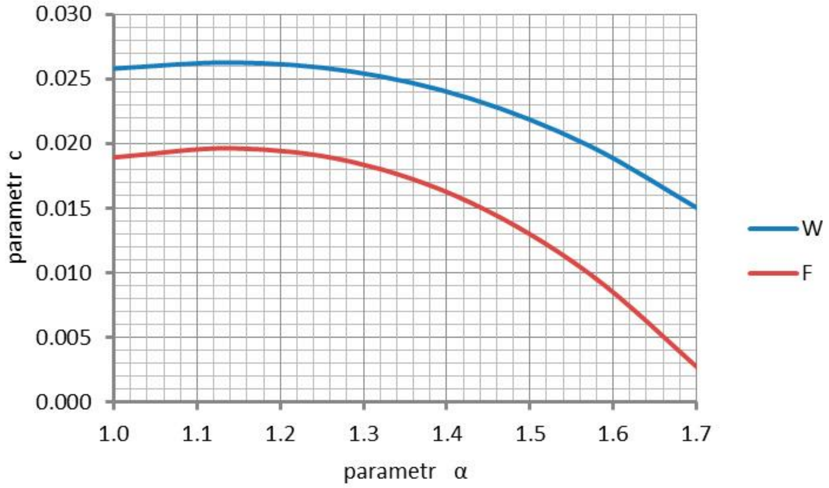

Figure 10. Displacement versus end span length.

Both the computational model shown in Figure 3 and the solution assume that there will be two double cantilevers made over support *j*. This means that in viaducts, i.e. multi-span systems with a repeatable structure, there occur repeatable span lengths $L = L_1 = L_2 = L_i$. Because of the symmetry one gets no rotation over the support, i.e. $\varphi = 0$. Consequently, for a larger number of spans built using the cantilever method a greatly simplified computational model is used. Thus, the deflection depends solely on the stiffness ratio represented by parameter n, as in formula (4). Figure 11 shows a diagram of the deflection. When $n = 1$, i.e. when haunches are absent, one gets

$$w = \frac{8}{192} \cdot \frac{qa^4}{EI} \qquad (13)$$

while when $n = 0.1$, the deflection diminishes to

$$w = \frac{2.44}{192} \cdot \frac{qa^4}{EI} \qquad (14)$$

The above example refers to the bridge shown in Figure 8, where the support is constructed as rigid. Such a system makes it impossible for angle of rotation φ (Figure 3) to form. Despite this constructional solution, the increment in deflection resulted in the excessive deflection of the main span. This case is analysed in detail in study [19].

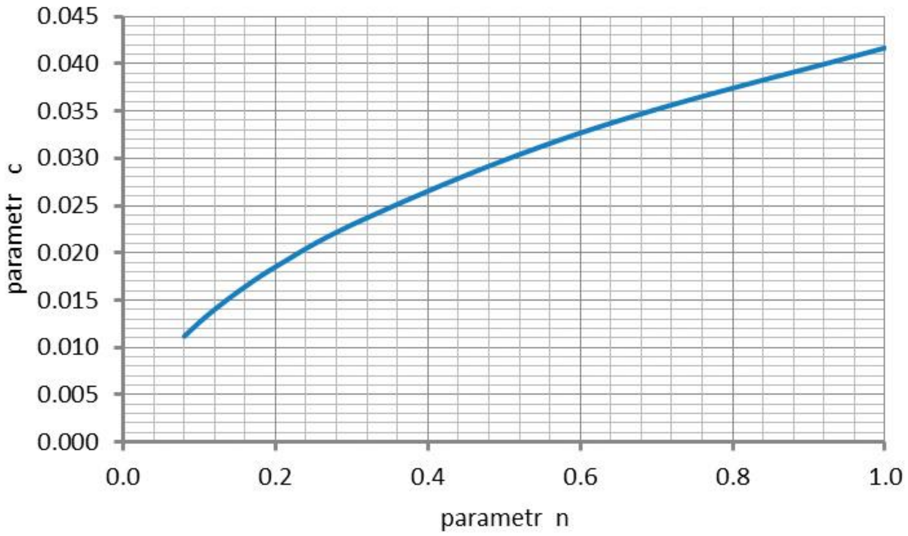

Figure 11. Deflection at midspan versus stiffness over support.

7. CONCRETE BRIDGE FLEXIBILITY FUNCTION

In this paper the maximum deflection (w) of the main span is analysed as resulting from the dead load in the form of a force with magnitude q, uniformly distributed along the whole length of the bridge. The flexibility of the bridge under the steady load is expressed as a ratio of the maximum deflection of the main span to the load, as in the formula

$$f = \frac{w}{q} = c_w \frac{a^4}{EI} \tag{15}$$

Thus the previously considered values of coefficient c_w from formula (1) are the bridge's characteristic (unfactored) static load values. The value of this coefficient takes into account the structural system of the bridge and the variation in the geometric parameters of the cross section along the length of the main span. For example, the flexibility of the bridge shown in Figure 1 for the results presented in Figure 10 at $\lambda = 75/70 = 1.07$ amounts to

$$f = 0.027 \frac{70^4}{43.72 \cdot 10^4} = 1.483 \quad [m^2/MN] \tag{16}$$

Span stiffness *EI=43,72*104* takes into account the bridge material. Parameter n takes into account the distribution of main girder stiffness and the load diagram covering span lengths L, L_1 and L_2. Whereas the value of f does not comprise the individual characteristics of the bridge. The unique cast-in place segmental construction and the phased prestressing of the segments are not taken into account. Of major importance are the rheological characteristics initiated by the bridge construction process.

The monitoring of the grade line of concrete spans [3, 8] reveals changes in deflection during the service life of the bridge (Figure 2). This means that *w(t)* is a function with time domain *t*. Under identical constant load g and q and at invariable span length *L* and moment of inertia *I(x)*, assuming slight changes in *E(t)*, the changes in bridge deflection can be expressed by the following compliance flexibilityfunction

$$f(t) = \frac{w(t)}{g+q} \tag{17}$$

where: *w(t)* – change of deflection of the mid span
g – dead load (self-weight)
q – uniformly distributed force (equipment)

Thus, the bridge flexibility is a time function. As a result of the primary prestressing (during construction) and the secondary prestressing (after joining the cantilevers together) of the bridge structure a marked reduction in deflection (caused by the dead load) occurs. According to formula (17) and the measurement results (Figure 2), the bridge's flexibility is subject to increase as a result of the rheological processes taking place in the concrete [1, 2, 13, 15, 17], especially as a result of the creep of the concrete [16, 19, 5]. Of major importance are the reduction in the prestress force and damage (cracking) to the concrete.

Measurements are usually conducted after secondary components are installed, i.e. after *q(t)* reaches its full value. This means that function *f(t)* is created beginning with the reference measurement when advanced rheological processes take place in the structure's concrete and prestressing steel as a result of the construction process. In the case of the analysed bridge (Figure 1), when on the basis of surveying measurements, one gets the deflection diagram as shown in Figure 12, after the weight of the secondary components(q) and the dead weight (g) are determined one can represent the change in the flexibility of the bridge. In the case of the considered exemplary bridge when $g = 0.231$ *MN/m and* $q = 0.035$ *MN/m*, from formula (17) one gets the value at the end measurement time

$$f(t_k) = \frac{w(t)}{q+g} = \frac{0.16}{0.266} = 0.6015 \quad [m^2/MN] \tag{18}$$

where: *w(t)* – change of deflection of the mid span
g – dead load (self-weight)
q – uniformly distributed force (equipment)

Since the measurements are performed on the bridge being in service, the value calculated above is related to the reference measurement. Hence when $w(t_o) = 0$, one also gets $f(t_o) = 0$. Function $f(t)$ is created on the basis of the results of measurements, but it can also be obtained through complicated computer simulations [18].

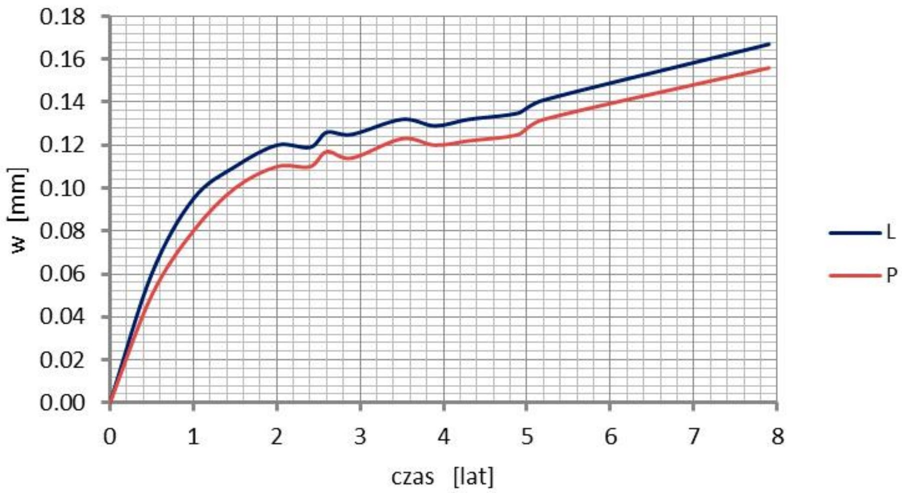

Figure 12. Deflection of bridge as in Figure 1 over time.

Considering formula (17), the graph of function $f(t)$ is similar to that of deflection $w(t)$ shown in Figure 12. This means that the two graphs represent the bridge's individual characteristics obtained from the bridge grade line measurement period. Graph $f(t)$ is similar to that of creep graph $C(t)$ and its values are influenced by the static system and the previously determined parameter c_w.

8. SUMMARY

Deflection w of the main span with length L under uniformly distributed load q was analysed in this paper. The basic variable parameter was the change in moment of inertia $I(x)$ along the length of the main span and the adjoining spans. Several structural systems used in bridges built using the cantilever (cast-in-place segmental construction) method were considered. Owing to the parametric form of the solution the results of the calculations also apply to other bridges. The results of the analyses presented in this paper can be used to reduce the rheological effects in designed concrete bridges.

The solution in form (1) provides the basis for formula (15) for bridge flexibility calculated using bridge load diagram characteristic value c_W. The calculated flexibility can be useful in analyses of long-term (rheological) changes in concrete bridge structures. It is a complement to the term bridge stiffness used in the case of momentary (short-term) loads, including dynamic actions.

Geodetic measurement techniques are useful for analysing the time-varying flexibility function. The analyses indicate that bridge monitoring results can be used in the case of bridges showing considerable deflections (as in Figure 2) right from the beginning of their service life. The deformation function is used to predict bridge deflections in the course of the further service life.

REFERENCES

[1]. Bazant Z., Guang-Hua Li, Qiang Yu, Klein G., Kristek V. , *Explanation of Excessive Long-Time Deflections of Collapsed Record-Span Box Girder Bridge in Palau. Preliminary report*, presented and distributed at the 8th International Conference on Creep and Shrinkage of Concrete. **2008**

[2]. Bažant Z., Hubler M.H., Glang Y., *Excessive Creep Deflections: An Awakening. Concrete International,* 8(33), 44-46. **2011**

[3]. Burdet O., *Experience in the Long-Term Monitoring* Bridges, 3rd fib International Congress, **2010**

[4]. Burdet O., and Badoux M., *Deflection monitoring of pre-stressed concrete bridges retrofitted by external post-tensioning*, IABSSE SYMPOSIUM RIO DE JANEIRO. **1999**

[5]. Kaklauskas G., Gribarnik V., Barcinskas D., Vainiunas P., *Schrinkage influence on tension stiffening in concrete members,* Engineering Structures 31 1305-1312 **2008**

[6]. Kalny M., Soucek P., Kvasnicka V., *Long-term behaviour of balanced cantilever bridges*. ACEB Workshop, Corfu. **2010**

[7]. Keijer U., *Long-term Deflections of Cantilever pre-stressed Concrete Bridges*, IABSE, No 5. **1970**

[8]. Kristek V., Vrablik L., Hrdousek V., *Causes of long-term deflections of large-span pre-stressed concrete box girders and recommendations on how to avoid those*. Transactions on Transport Sciences, Volume 1, Number 3,. **2008**

[9]. Machelski C., Pisarek B., *Change of the grade line of bridges constructed with cantilever concreting technology*, Journal of Architecture Civil Engineering Environment, 4/2017, 2, 65-72. **2017**

[10]. Morlova D., Chiotan C.: *Monolithic concrete vs precast concrete for the construction of bridge in by the cantilever method*. Romanian Journal of Transport Infrastructure Vol.4, No.1 **2015**

[11]. Navratil J., Zich M., *Long-Term Deflections of Cantilever Segmental Bridges.* The Baltic Journal of Road and Bridge Engineering. 8(3): 190-195. **2013**

[12]. Pisarek B., *Analyse of the grade line and the rheological effects in the bridges constructed with cantilever method*, Young Engineering Colloquium, Berlin, 66-68. **2019**

[13]. Pisarek B., Machelski C.: *Estimation of rheological effects in cantilever concrete bridges on the basis of spandeflection line*. Periodica Politechnica Civil Engineering. 66(1) pp. 228-234 **2022**

[14]. Pisarek B. Machelski C., *Rheological effects in the bridges constructed with cantilever method*, Romanian Journal of Transport Infrastructure, Article No.5, Vol9, 2020, No.1 **2020**

[15]. Rusch J., *Stahlbeton - Spannbeton Band 2: Berücksichtigung der Einflüsse von Kriechen und Schwinden auf das Verhalten der Tragwerke*. **1976**

[16]. Smith M.J., Goodyear D., *A Practical Look at Creep and Shrinkage in Bridge Design*, PCI Journal, May-June, 108-121. **1988**

[17]. Takacs P.F., *Deflections in Concrete Cantilever Bridges: Observation and Theoretical Modelling*, Doctoral Thesis, Trondheim. **2002**

[18]. Tang Man-Chung: *The Story of the Koror Bridge*. IABSE Bulletins **2014**.

[19]. Tong T., Wendner R., Strauss A., Wang W., Yu Q., *Effects of concrete creep and its randomness on long-term deflection of prestressed box grider*. 4th International Symposium on Life-Cycle Civil Engineering, Tokio. **2014**

[20]. Trost H, *Zur Berechnung von Stahlverbundträgern im Gebrauchszustand auf Grund neuerer Erkenntnisse des viskoelastischen Verhaltens des Betons*, Der Stahlbau, 11, 321-331. **1968**

[21]. Wendner R., Tong T., Strauss A., Yu Q., *A Case Study on Correlations of Axial Shortening and Deflection with Concrete Creep Asymptote in Segmentally-Erected Prestressed Box Girders*, Structure and infrastructure Engineering, Januar **2015**